Investigation of Solid and Solution Structures of N-Substituted Cu(II) Salicyldimines by X-Ray Absorption Spectroscopy

Michael D. Wirt,*,† Luigi Bubacco,‡ and Jack Peisach*,†,‡

Department of Molecular Pharmacology and Department of Physiology and Biophysics, Albert Einstein College of Medicine, 1300 Morris Park Avenue, Bronx, New York 10461

Received July 22, 1994[⊗]

A series of bis(*N*-alkylsalicylaldiminato)copper(II) complexes that serve as models for mononuclear, nontetragonal copper(II) sites in copper proteins are examined by X-ray absorption spectroscopy in order to investigate their structural characteristics in crystalline, room temperature solution, and frozen solution forms. Previous electron paramagnetic resonance (EPR) studies of frozen solution samples of bis(*tert*-butylsalicylaldiminato)copper(II) (Cu^{II}(*t*-butSal)$_2$) suggest solvent dependent variation in site symmetry (Rosenberg; *et al. J. Am. Chem. Soc.* **1975**, *97*, 2092). In addition, linear electric field effect (LEFE) investigations in frozen solution reveal a deviation from centrosymmetry greater than expected based on the X-ray crystal structure (Peisach and Mims, *Eur. J. Biochem.* **1978**, *84*, 207). X-ray edge results indicate that a more tetrahedral coordination geometry is assumed by Cu^{II}(*t*-butSal)$_2$ in solution preparations, both at room temperature or frozen, when compared with crystalline samples. Extended X-ray absorption fine structure (EXAFS) studies of the Cu^{II}(*t*-butSal)$_2$ species show no difference in metal–ligand distances between crystalline or frozen solution samples. In contrast, no differences in X-ray edge spectra were detected between crystalline and solution forms of bis(methyl- and bis-(propylsalicylaldiminato)copper(II) complexes nor for bis(salicylaldehyde)copper(II), which suggests that bulkiness of the *N*-alkyl group in salicyldimines mediates the geometric sensitivity to local environmental conditions.

Introduction

An issue raised by structural determinations based on X-ray crystallographic analysis is whether the structure obtained for a complex in the crystalline state is the same as that for the complex in solution. In some instances, it has been found that crystal packing forces or aggregation during crystallization can distort structures; for example, these phenomena have been cited for solid and solution structural studies of both metallothionine-2[1,2] and the polypeptide hormone glucagon.[3] Additionally, recent EXAFS studies of crystalline and solution forms of metmyoglobin[4] and concanavalin A[5,6] both report differences in average first coordination sphere metal–ligand distances. Further, for concanavalin A, changes in coordination number of the bound metal are observed when comparing the crystalline and solution structures.[6] Consequently, considerable interest remains in comparing chemical structures in the solid state and solution. Therefore, we have employed X-ray absorption spectroscopy (XAS) to further investigate the structure of transition metal complexes in both the solid state and in solution. Many techniques used for structural determination have phase and temperature limitations. X-ray edge spectroscopy does not suffer from these limitations and materials can be examined in solution as well as in the solid state.

In this study, we have examined a series of bis(*N*-alkylsalicylaldiminato) copper(II) complexes that model mononuclear, nontetragonal copper(II) sites in copper proteins, such as stellacyanin,[7] in order to investigate their structural characteristics in crystalline, room temperature solution, and in frozen solution forms. We present data obtained from both X-ray edge and extended X-ray absorption fine structure (EXAFS) spectroscopy that demonstrate structural differences in the crystalline and solution conformations of bis(*tert*-butylsalicylaldiminato)-copper(II) (Cu^{II}(*t*-butSal)$_2$). Earlier crystallographic studies of Cu^{II}(*t*-butSal)$_2$ by Cheeseman *et al.*[8] indicate a distorted tetrahedral conformation where the dihedral angle between the two salicyldimine planes (each encompassing the copper, one oxygen and one nitrogen ligand) is ca. 54° due to the presence of the bulky *tert*-butyl substituent[8–11] (Figure 1). In addition, linear electric field effect (LEFE) studies at low temperature indicate a greater deviation from tetragonal symmetry than expected from the X-ray crystal structure.[12] In contrast, electron paramagnetic resonance (EPR) studies of frozen solution samples exhibit solvent dependent variations in magnetic parameters which have been interpreted to represent a variation in deviation from tetragonal symmetry.[13]

In this investigation, our X-ray edge results indicate that a more tetrahedral coordination geometry is assumed in both frozen solution and room temperature solution preparations of the Cu^{II}(*t*-butSal)$_2$ complex when compared with the crystalline material. In contrast, no distinct differences in X-ray edge

† Department of Molecular Pharmacology.
‡ Department of Physiology and Biophysics.
⊗ Abstract published in *Advance ACS Abstracts,* April 1, 1995.

(1) Vasak, M.; Worgotter, E.; Wagner, G.; Kagi, J. H. R.; Wuthrich, K. *J. Mol. Biol.* **1987**, *196*, 711.
(2) Schultze, P.; Worgotter, E.; Braun, W.; Wagner, G.; Vasak, M.; Kagi, J. H. R.; Wuthrich, K. *J. Mol. Biol.* **1988**, *203*, 251.
(3) Bosch, C. H.; Bundi, A.; Oppliger, M.; Wuthrich, K. *Eur. J. Biochem.* **1978**, *91*, 209.
(4) Zhang, K.; Chance, B.; Reddy, K. S.; Ayene, I.; Stern, E. A.; Bunker, G. *Biochemistry* **1991**, *30*, 9116.
(5) Lin, S. L.; Stern, E. A.; Kalb (Gilboa), A. J.; Zhang, Y. *Biochemistry* **1991**, *30*, 2323.
(6) Lin, S. L.; Stern, E. A.; Kalb (Gilboa), A. J.; Zhang, Y. *Biochemistry* **1990**, *29*, 3599.
(7) Peisach, J.; Powers, L. S.; Blumberg, W. E.; Chance, B. *Biophys. J.* **1982**, *38*, 277.
(8) Cheeseman, T. P.; Hall, D.; Waters, T. N. *J. Chem. Soc. A* **1966**, 685.
(9) Bombieri, G.; Panattoni, C.; Fursellini, E.; Graziani, R. *Acta Crystallogr., Sect. B* **1969**, *25*, 1208.
(10) Wei, L.; Strogsdill, R. M.; Lingafelter, E. C. *Acta Crystallogr., Sect. B* **1964**, *17*, 1058.
(11) Orioli, P. L.; Sacconi, L. *J. Am. Chem. Soc.* **1966**, *88*, 277.
(12) Peisach, J.; Mims, W. B. *Eur. J. Biochem.* **1978**, *84*, 207.
(13) Rosenberg, R. C.; Root, C. A.; Bernstein, P. K.; Gray, H. B. *J. Am. Chem. Soc.* **1975**, *97*, 2092.

0020-1669/95/1334-2377$09.00/0

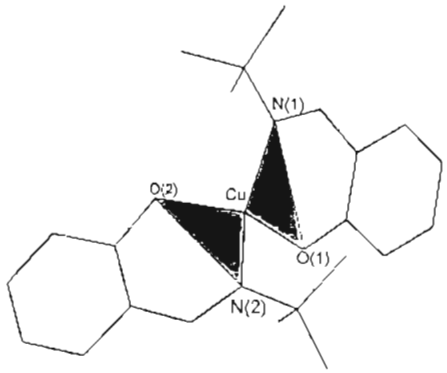

Figure 1. Structure of bis(*N*-*tert*-butylsalicylaldiminato)copper(II). Plane 1 consists of the copper atom, N(1), and O(1), while plane 2 contains copper, N(2), and O(2). The dihedral angle ($\alpha = 54°$) is defined by the intersection of the two planes at the copper center. A dihedral angle of 0° indicates a planar conformation, and an angle of 90° a perfect tetrahedral geometry. The structure was drawn using data obtained from the Cambridge Crystallographic Data Base (version 5).[36]

spectra were detected between crystalline, frozen solution and room temperature solution preparations of bis(methyl- and bis-(propylsalicyldimine)copper(II) ($Cu^{II}(meSal)_2$, $Cu^{II}(prSal)_2$) or bis(salicylaldehyde)copper(II) ($Cu^{II}(salald)_2$). EXAFS studies on the $Cu^{II}(t\text{-butSal})_2$ species show no change, within the error of the measurements, in metal−ligand distances for the crystalline or frozen solution samples.

Materials and Methods

Methods. (5,10,15,20-Tetraphenyl-21*H*,23*H*-porphine)copper(II), ($Cu^{II}TPP$) was purchased from Aldrich Chemical Co. and was used without further purification. The bis(*N*-alkylsalicylaldiminato)copper-(II) complexes were prepared as described previously.[14] All salicyldimine samples were recrystallized in cyclohexane and dried under vacuum. Optical absorption properties, EPR spectra, and melting point determinations were consistent with published data for all samples.[8,13-17] Anal. Calcd (Schwarzkopf Microanalytical Lab Inc.) for the *tert*-butylsalicyldimine complex: C, 63.5; H, 6.8; N, 6.7. Found: C, 62.3; H, 6.5; N, 6.7. Room temperature and frozen solution XAS samples (120 K) were prepared in methanol/chloroform 1:1 (v/v) mixtures for direct comparison to previous LEFE experiments of Peisach *et al.*[12] In order to minimize fluorescence saturation effects in the XAS experiments, crystalline samples were diluted to ca. 0.5 wt % copper in aluminum oxide and ground to a fine powder in a mortar and pestle to insure uniformity. All samples were placed in 25 × 2.5 × 2 mm deep Lucite sample holders covered with Kaypton tape.

Data Collection

X-ray fluorescence data were collected at the National Synchrotron Light Source (NSLS), Brookhaven National Laboratory, on beam lines X-9A and X-10C, using double flat Si(111) (X-9A) and Si(220) (X-10C) crystal monochromators with fixed exit geometry. Beam harmonics were rejected by using a nickel (X-9A) or rhodium (X-10C) coated mirror positioned down stream of the monochromator. Sample temperature was maintained by flowing cooled nitrogen gas through a Lucite cryostat as described previously.[18] X-ray edge data having 3 eV resolution (X-9A) and 2 eV resolution (X-10C) were recorded by counting at one energy value for 3 s and incrementing the energy in 0.5 eV steps from 30 eV below the copper edge to 120 eV above the edge. EXAFS data were collected by counting at a specific energy for 1 s and incrementing the energy by 10 eV from 100 eV below the copper edge to 20 eV below the edge, then in 2 eV steps (2 s per point) to 20 eV above the edge, in 3 eV steps for 4 s per point to 400 eV above the edge, and finally by increasing counting time to 6 s per point from 400 to 1000 eV above the edge. Five EXAFS scans were collected for each solid and solution $Cu^{II}(t\text{-butSal})_2$ sample. Copper foil was used as an energy standard to account for any shifts in the monochromator calibration. Kaypton tape was mounted at a 45° angle to the incident X-ray beam to scatter X-ray photons through the copper foil. The photons were then counted with a photomultiplier tube positioned perpendicular to the X-ray beam. X-ray flux was 1.0×10^{10} photons s^{-1} mm^{-2} at 100 ma beam current (X-9A) and 1.3×10^{10} photons s^{-1} mm^{-2} at 100 ma beam current (X-10C). Both X-ray edge and EXAFS data were generally taken in the range of 100-225 ma. Kα copper fluorescence was detected with a 13-element solid-state energy resolving germanium detector and incident photon scattering was rejected by a nickel filter. Reference signals (incident beam intensity, I_0) were collected using a standard ion chamber.

Table 1. Integrated Areas for 1s−3d and 1s−4p + Shake-Down (SD) Transition Intensities for Bis(*N*-alkylsalicylaldiminato)copper(II) and Model Complexes[a]

compd	sample conditions	1s−3d intens	1s−4p + SD intens
$Cu^{II}(t\text{-butSal})_2$	298 K, solution	0.056 ± 0.006	0.127 ± 0.005
$Cu^{II}(t\text{-butSal})_2$	120 K, frozen solution	0.048 ± 0.003	0.197 ± 0.002
$Cu^{II}(t\text{-butSal})_2$	crystalline	0.032 ± 0.002	0.377 ± 0.003
$Cu^{II}TPP$	crystalline	0.005 ± 0.001	0.672 ± 0.004
$Cu^{II}(prSal)_2$	298 K, solution	0.014 ± 0.002	- - -
$Cu^{II}(prSal)_2$	crystalline	0.020 ± 0.006	- - -
$Cu^{II}(meSal)_2$	298 K, solution	0.021 ± 0.002	- - -
$Cu^{II}(meSal)_2$	crystalline	0.016 ± 0.002	- - -
$Cu^{II}(salald)_2$	298 K, solution	0.015 ± 0.009	- - -
$Cu^{II}(salald)_2$	crystalline	0.013 ± 0.008	- - -

[a] Integrated areas for pre-edge transitions are presented in eV, where the edge jump has been normalized to 1.0 (see text). Dashed entries indicate that no 1s−4p + SD transition was observed for that complex.

Data Analysis and Errors

X-ray edge data were converted to two column ASCII format and then processed using the Galactic Industries *Spectra Calc* (1988) software package. Edge spectra were normalized by fitting a best line to pre- and post-edge regions of the spectrum and normalizing the edge jump to 1.0 at 9060 eV. Pre-edge features were integrated for comparison as described previously.[19,20]

Two factors contributed to the estimated errors: those due to statistical noise and those inherent to the method of analysis. Statistical noise was measured in the linear region prior to the edge. Contributions of statistical noise to integrated pre-edge peak areas were determined by calculating the percent contribution of the statistical noise to the total peak area. This provided a measure for the statistical error of each scan (which varied between 1% and 15% depending on the transition intensity, sample concentration, beam conditions, and signal averaging). Errors inherent to the method of analysis were calculated by comparison of integrated areas of different scans for the same sample. These systematic errors were generally ≤0.5%. Errors seen in Table 1 represent the error of the measurement taking into consideration the statistical and systematic errors discussed above.

EXAFS Data Analysis and Errors. Data Analysis. EXAFS background removal, k^3-weighing, Fourier filtering, and nonlinear least-squares procedures followed standard methods.[21-23] Raw, deglitched data for crystalline and frozen solution $Cu^{II}(t\text{-butSal})_2$ samples were used for the EXAFS analysis. Background subtracted data were Fourier transformed using square window functions. The Fourier filter back-

(14) Sacconi, L.; Campolini, M. *J. Chem. Soc. A* **1964**, 276.
(15) Cheeseman, T. P.; Hall, D.; Waters, T. N. *J. Chem. Soc. A* **1966**, 694.
(16) Yokoi, Y. *Bull. Chem. Soc. Jpn.* **1974**, *47*, 3037.
(17) Bertini, I.; Canti, G.; Grassi, R.; Scozzafava, A. *Inorg. Chem.* **1980**, *19*, 2198.
(18) Powers, L. S.; Chance, B.; Ching, Y.; Angioillo, P. *Biophys. J.* **1981**, *34*, 465.
(19) Wirt, M. D.; Sagi, I.; Chen, E.; Frisbie, S. M.; Lee, R.; Chance, M. R. *J. Am. Chem. Soc.* **1991**, *113*, 5299.
(20) Wirt, M. D.; Chance, M. R. *J. Inorg. Biochem.* **1993**, *49*, 265.
(21) Sagi, I.; Wirt, M. D.; Chen, E.; Frisbie, S. M.; Chance, M. R. *J. Am. Chem. Soc.* **1990**, *112*, 8639.
(22) Chance, M. R.; Powers, L. S.; Kumar, C.; Chance, B. *Biochemistry* **1986**, *25*, 1259.
(23) Lee, P.; Citrin, P.; Eisenberger, P.; Kincaid, B. *Rev. Mod. Phys.* **1981**, *53*, 769.

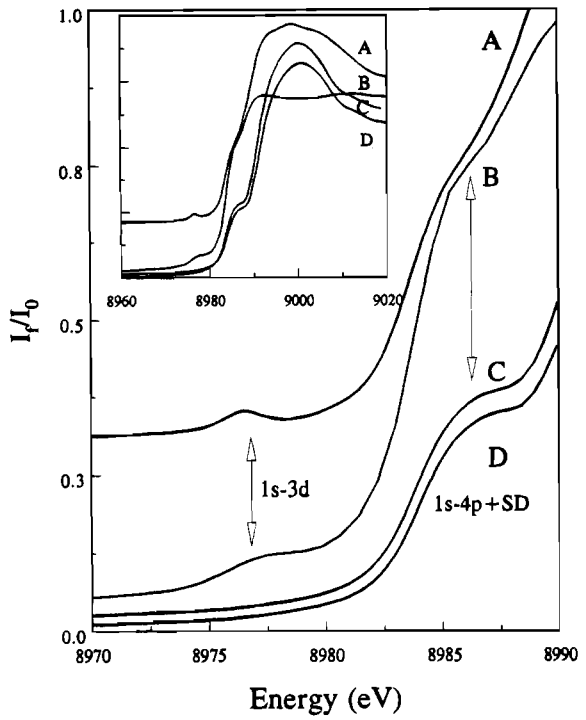

Figure 2. X-ray fluorescence edge data of $Cu^{II}TPP$ and $Cu^{II}(t\text{-butSal})_2$ under varying sample conditions: (A) $Cu^{II}(t\text{-butSal})_2$, frozen solution, 1s−3d and 1s−4p + SD, distorted tetrahedron; (B) $Cu^{II}(t\text{-butSal})_2$, crystalline, 1s−3d and 1s−4p + SD, distorted (flattened) tetrahedron;[2] (C) $Cu^{II}TPP$, crystalline, 1s−4p + SD, square planar;[11] (D) $Cu^{II}TPP$, frozen solution, 1s−4p + SD, square planar. Comparison of frozen solution X-ray edge spectra of $Cu^{II}(t\text{-ButSal})_2$ with spectra collected at room temperature show small differences in integrated pre-edge transition areas (Table 1). Spectra have been arbitrarily offset to ease comparison.

transform (r-window) function limits were set to $r_1 = 1.0$ and $r_2 = 2.2$ Å for both crystalline and solution samples. Data were Fourier transformed with 0.2 to 11.3 $Å^{-1}$ in k-space. The Fourier filtered, back-transformed data were then fit from 4.0 to 11.0 $Å^{-1}$ in k-space. EXAFS parameters were obtained by fitting $Cu^{II}(t\text{-butSal})_2$ data to $Cu^{II}TPP$ model data using the AT&T Bell Laboratories EXAFS Package.[24] Cu^{II}-TPP model compound data were processed the same way as detailed above.

Errors. Errors in the EXAFS analysis were estimated by three methods. To determine the degree of statistical or random noise, partial sums of the total number of scans were independently fit. The differences in the fit distances provide an estimation of random noise. Second, systematic errors due to variations in sample preparation and beam fluctuations were estimated by separate analysis of independently prepared samples. Third, the method of mapping the minimum solution by examination of χ^2 (sum of residuals squared) was applied.[25] Errors ranged from ±0.01−0.02 Å for distances.

Results and Discussion

X-ray Edge Spectroscopy. X-ray edge spectra of crystalline and frozen solution samples of $Cu^{II}(t\text{-butSal})_2$ are presented in Figure 2. $Cu^{II}TPP$ provides an excellent square-planar model for comparison. X-ray diffraction data indicates that the first coordination sphere of $Cu^{II}TPP$ contains four nitrogen ligands with mean deviations from the porphyrin plane of only 0.04Å.[26] For this compound, no differences in pre-edge X-ray absorption intensities are detected between crystalline and solution preparations (Figure 2). Additionally, LEFE studies of $Cu^{II}TPP$ in frozen solution indicate an essentially centrosymmetric coordination environment,[12] making it an ideal reference complex.

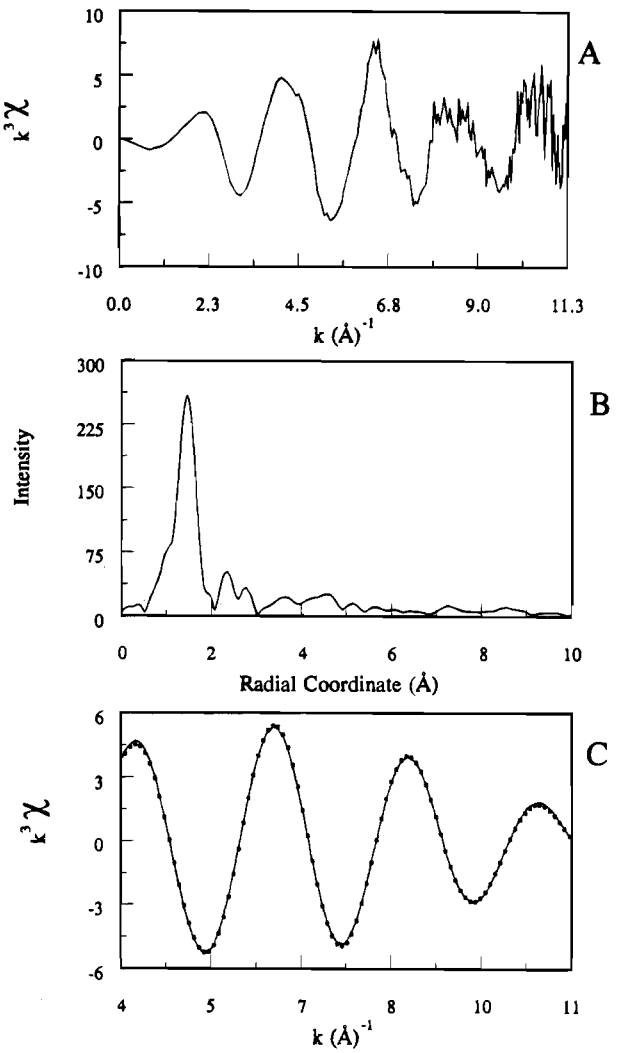

Figure 3. (A) Deglitched, wavevector cubed, background subtracted data of Cu(II) bis(*tert*-butylsalicyldimine) ($Cu^{II}(t\text{-butSal})_2$) in frozen solution. Data were Fourier transformed from 0.2 to 11.3 $Å^{-1}$ in k-space. (B) Fourier transform of the background subtracted data presented in Figure 3A. (C) Back-transformed data of $Cu^{II}(t\text{-butSal})_2$ (solid lines) compared with the two-atom simulation (E, Table 2) (squares): $\chi^2 = 0.3$. Data are fit from 4.0 to 11.0 $Å^{-1}$ in k-space.

The presence of a strong 1s−4p + shake-down (transfer of charge from ligand to metal, (SD)) transition, observed for Cu^{II}-TPP (seen as a shoulder on the absorption edge, see inset, Figure 2), is indicative of square planar geometry.[27,28] Distortions from planar geometry would reduce the 1s−4p + SD transition intensity as a consequence of a decreased interaction between ligand and metal orbitals.

Comparison of the $Cu^{II}TPP$ edge spectrum to that of $Cu^{II}(t\text{-butSal})_2$ in the crystalline state (Figure 2) shows an approximate 2-fold decrease in the 1s−4p + SD transition intensity. These results are consistent with the distorted tetrahedral structure observed by Cheeseman *et al.* in the X-ray crystal structure.[8] Further, comparison of the crystalline $Cu^{II}(t\text{-butSal})_2$ species with both the frozen and room temperature solution samples demonstrates a significant change in geometry concurrent with phase change. The ca. 60% increase in 1s−3d transition intensity and ca. 30% reduction in 1s−4p + SD transition intensity for room temperature solution X-ray edge spectra indicate a more tetrahedral geometry for the structure in solution.[28−30] These results are consistent with earlier low

(24) Scheuring, E.; Sagi, I.; Chance, M. R. *Biochemistry* **1994**, *33*, 6310.
(25) Lytle, F. W.; Sayers, D. E.; Stern, E. A. *Phys. B* **1989**, *158*, 701.
(26) Fleischer, E. B. *J. Am. Chem. Soc.* **1963**, *85*, 1353.
(27) Bair, R. A.; Goddard, W. M. *Phys. Rev. B* **1980**, *22*, 2767.
(28) Kosugi, N.; Yokoyama, T.; Kuroda, H. *Chem. Phys.* **1986**, *104*, 449.

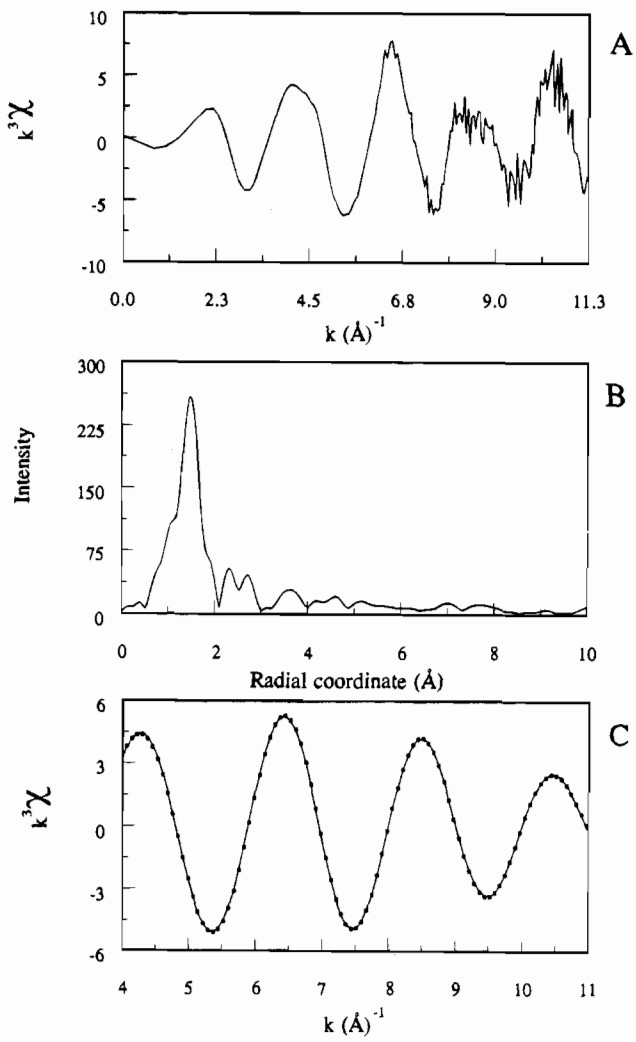

Figure 4. (A) Deglitched, wave-vector cubed, background subtracted data of crystalline copper(II) bis(*tert*-butylsalicyldimine) (Cu^{II}(*t*-butSal)$_2$). Data were Fourier transformed from 0.2 to 11.3 Å^{-1} in *k*-space. (B) Fourier transform of the background subtracted data presented in Figure 4A. (C) Back-transformed data of Cu^{II}(*t*-butSal)$_2$ (solid lines) compared with the two-atom simulation (J, Table 2) (squares); χ^2 = 0.05. Data were fit from 4.0 to 11.0 Å^{-1} in *k*-space.

temperature LEFE studies by Peisach and Mims.[12,31] where the Cu^{II}(*t*-butSal)$_2$ complex in frozen solution was found to have an unusually large distortion from tetragonal geometry compared with that observed in the crystal structure.[8] Additionally, smaller, but significant differences are also observed when comparing integrated pre-edge transition areas from frozen solution and room temperature samples (Table 1).

No distinct differences in pre-edge transition intensities were detected between crystalline and solution forms of Cu^{II}(meSal)$_2$, Cu^{II}(prSal)$_2$, or Cu^{II}(salald)$_2$ complexes (Table 1), which suggests that the bulkiness of the alkyl group mediates the geometric sensitivity to local environmental conditions. Copper(II) bis(methyl- and bis(propylsalicyldimine) as well as copper(II) bis(salicylaldehyde) spectra contain 1s−3d transitions with intensities consistent with a weakly distorted tetragonal species as reported earlier.[8−12]

(29) Bart, C. *Adv. Catal.* **1986**, *24*, 203.
(30) Roe, A. L.; Schneider, D. J.; Mayer, R. J.; Pyrz, J. W.; Widom, J.; Que, L., Jr., *J. Am. Chem. Soc.* **1984**, *106*, 1676.
(31) A LEFE study of crystalline Cu^{II}(*t*-butSal)$_2$ would be desirable for a final comparison. Difficulties in finding a suitable host lattice to provide a magnetically dilute crystalline material that does not impose geometric distortions on the Cu(II) salicyldimine have precluded this effort. Previous continuous wave EPR[17] and X-ray diffraction[35] studies of bis(*N*-alkylsalicylaldiminato)zinc(II) complexes containing 1% doping of the analogous Cu(II) complex show that the doped Cu(II) complex assumes the pseudotetrahedral conformation of the zinc lattice.

Table 2. Nonlinear Least-Squares Fitting Results for Crystalline and Solution Preparations of Bis(*tert*-butylsalicylaldiminato)copper(II) EXAFS Spectra[a]

fit type	solution	model	*N*	*r* (Å)	ΔE_o (eV)	$\Delta\sigma^2$ (Å^2)	χ^2
			Frozen Solution				
1-atom	A	Cu−N	6.0	1.95	1.76	$+4 \times 10^{-3}$	23.0
	B	Cu−N	5.0	1.95	1.82	$+3 \times 10^{-3}$	14.9
	C	Cu−N	4.0	1.95	1.70	$+2 \times 10^{-3}$	3.2
	D	Cu−N	3.0	1.95	1.60	-6×10^{-4}	26.7
2-atom	E	Cu−N	2.1	1.98	1.18	-8×10^{-5}	0.3
		Cu−N	2.2	1.90	4.33	-3×10^{-3}	
			Crystalline				
1-atom	F	Cu−N	6.0	1.96	−0.88	$+5 \times 10^{-3}$	43.5
	G	Cu−N	5.0	1.96	−0.93	$+3 \times 10^{-3}$	19.1
	H	Cu−N	4.0	1.96	−1.04	$+1 \times 10^{-3}$	7.2
	I	Cu−N	3.0	1.96	−1.21	-1×10^{-3}	17.1
2-atom	J	Cu−N	1.9	1.98	1.53	-5×10^{-3}	0.05
		Cu−N	2.1	1.87	2.19	-4×10^{-4}	

[a] One and two-atom type solutions result from fixing coordination number (*N*), and allowing the metal−ligand distance (*r*), Debye−Waller factor ($\Delta\sigma^2$), and threshold energy (ΔE_o), the latter with two respect to the model compound, float to minimize χ^2. Back-transformed data are fit to Cu^{II}TPP (4Cu−N at 1.981 Å average distance).[26] Best fit solutions for the two Cu^{II}(*t*-butSal)$_2$ species lie in a well-defined minimum located at ca. 4 ligands.

EXAFS. Figures 3A and 4A show the raw wavevector cubed and background subtracted data for the frozen solution and crystalline forms of Cu^{II}(*t*-butSal)$_2$, respectively. The Fourier transforms of the raw data in Figures 3A and 4A are presented in Figures 3B and 4B. Two-atom fits where distance (*r*), Debye−Waller factor shift ($\Delta\sigma^2$), and edge energy shift (ΔE_0) (the latter two with respect to the model compound) are allowed to vary, and coordination number (N) is fixed, are presented in Table 2 and Figures 3C and 4C. The two-atom fit for the frozen solution form of the Cu^{II}(*t*-butSal)$_2$ species gives a best solution of 2.1 nitrogen or oxygen type ligands at 1.98 ± 0.02 Å and 2.2 nitrogen or oxygen type ligands at 1.90 ± 0.02 Å, χ^2 = 0.3. The corresponding two-atom fit for the crystalline form gives a best fit solution of 1.9 nitrogen or oxygen type scatterers at 1.98 ± 0.01 and 2.1 nitrogen or oxygen type scatterers at 1.87 ± 0.01 Å, χ^2 = 0.05. The EXAFS results for the crystalline Cu^{II}(*t*-butSal)$_2$ are in good agreement with average metal−ligand distances of 1.985 ± 0.006 (Cu−N) and 1.898 ± 0.006 (Cu−O) determined by X-ray diffraction.[8]

Metal−ligand distances determined by EXAFS for the two Cu^{II}(*t*-butSal)$_2$ preparations are indistinguishable within the error of the measurements. However, examination of the radial distribution functions for frozen solution and crystalline preparations show subtle differences in second shell scattering amplitudes (located between 2 and 3 Å) which may be derived from contributions of *N*-*tert*-butyl substituents to the second shell backscattering profile. It is possible that these differences correlate with changes observed in the X-ray edge spectra as the geometry shifts toward more tetrahedral in solution. A similar change in the radial distribution function has been observed in a study of solvated solid and solution Cu(II) ion in bentonite clay, where the coordination number and geometry shifts from four-coordinate (square-planar) to six-coordinate (octahedral) upon exposure to excess solvent.[32]

Conclusions

XAS has been employed previously to study simple Cu(II) complexes in the solid state and solution.[32−34] Though X-ray

(32) Carrado, K. A.; Wasserman, S. R. *J. Am. Chem. Soc.* **1993**, *115*, 3394.

edge spectra have been reported for a portion of these complexes,[32-33] they have not been examined rigorously. Integration of normalized pre-edge transitions facilitates a means for semiquantitative analysis of X-ray edge spectra that is sensitive to variations in coordination geometry for samples collected under both solution and crystalline conditions. Thus, direct comparison of XAS data collected from metalloprotein samples under physiological conditions to those of crystalline solids can be achieved. A further advantage of the X-ray absorption technique is the ability to study crystalline samples without the requirement of doping the metal of interest in a host lattice as is usually required for EPR studies. This is a significant advantage, since doping often carries a risk of inducing structural alterations on the doped species by the host lattice. Additional model compound studies using the EXAFS technique will provide the database necessary for a more comprehensive method of second shell analysis of copper(II) salicyldimines.

Acknowledgment. This research is supported by National Institutes of Health Grants RR-02583 and GM-40168 (J.P.). We thank Mike Sullivan for technical assistance at beamline X-9A and Mike Sansone at beamline X-10C. The construction and operation of beamline X-9A is supported by National Institute of Health Grant RR-01633 and National Science Foundation Grant DMR-85190959. The National Synchrotron Light Source is supported by the U.S. Department of Energy, Division of Materials Sciences and Division of Chemical Sciences.

IC9408720

(33) Nomura, M.; Yamaguchi, T. *J. Phys. Chem.* **1988**, *92*, 6157.
(34) Beagley, B.; Eriksson, A.; Lindgren, J.; Persson, I.; Pettersson, L. G. M.; Sandstrom, M.; Wahlgren, U.; White, E. W. *J. Phys.: Condens. Matter* **1989**, *1*, 2395.
(35) Sacconi, L.; Ciampolini, M. *Ric. Sci. Rend.* **1962**, *32*, 645.
(36) Allen, F. H.; Kennard, O.; Taylor, R. *Acc. Chem. Res.* **1983**, *16*, 146.